Corrosion Resistance and Microstructure of Electrolytic Zinc Composite Coatings

Frank Fontenay, Per Møller and Lasse B. Andersen, Department of Manufacturing Engineering, Technical University of Denmark, Lyngby, Denmark.

Electrolytic zinc composite coatings are deposited from both sulfate and chloride-based acid baths. Metal hydroxides/oxides of primarily aluminum and chromium are codeposited as a result of a rising pH value in the catholyte. The codeposition is achieved by means of reduction of nitrate to ammonium in the solution.

The corrosion resistance of the zinc deposits is evaluated from both neutral salt spray testing and electrochemical tests.

The microstructure of the deposits is characterized by scanning electron microscopy combined with energy-dispersive X-ray analysis (EDS).

For more information, contact:

Frank Fontenay
Department of Manufacturing Engineering
Kemitorvet
DTU Building 204
2800 Kgs. Lyngby
Denmark

Phone: +45 45 25 22 12
Fax: +45 45 93 62 13
Email: fsf@ipt.dtu.dk

Introduction

In the last three decades, much effort has been given to the development of better electrolytic zinc and zinc alloy coatings. Though the research has resulted in the development of a vast amount of possible processes for alloy deposition, only a handful of these has found widespread use. The automotive industry has been a major driving force for the introduction of zinc-nickel, zinc-iron and zinc-cobalt on the market.

Zinc Alloy Plating

Zinc-nickel (5-15 % Ni) is primarily used by the automotive industry for under the hood applications and has an excellent corrosion resistance in neutral environment, even after heat treatment, as baking does not destroy the chromate.
Zinc-iron (up to 25 % Fe) is used for coil coating in the automotive industry because of its high ductility and weldability.
Zinc-cobalt (<1 % Co) is used mainly for fasteners and often in aggressive environments because of its superior corrosion resistance when exposed to acid and especially sulfur dioxide.[1-4]

The protection mechanism of especially zinc-cobalt has been the subject of numerous speculations and investigations, because the small amount of cobalt is insufficient to cause an ennoblement of the coating. Some suggested explanations are:

1. A changing of the semiconducting properties of the passive film.[5]
2. A formation of cobalt "electron traps".[6]
3. Small distortions of the zinc lattice caused by the cobalt atoms.[7]

Another question is that of the oxidation state of cobalt in the alloy coatings. Leidheiser et Al.[6, 8] have shown that cobalt as an oxidized species (e.g. an oxide) acts as a corrosion inhibitor on zinc. In that case, the surface zinc-cobalt layer could actually be classified as a composite rather than as an alloy coating.

Zinc Composite Coatings

Zinc composite coatings offer an alternative way of achieving improved corrosion resistance of zinc electro-coatings, namely by the codeposition of small amounts of non-metallic substances, typically hydroxides or oxides of metals.
An example of this is the codeposition of up to four weight-percent of aluminum, chromium and titanium in the form of hydroxides. These metals are either difficult or impossible to electrodeposit from aqueous solutions, so the codeposition takes place by the reduction of nitrate to ammonium at the cathode. The proposed reaction schemes are as follows:

$$\mathrm{Zn}^{2+} + 2\mathrm{e}^{-} \rightarrow \mathrm{Zn(s)} \qquad (1)$$

$$\mathrm{NO}_3^- + 6\mathrm{H}_2\mathrm{O} + 8\mathrm{e}^- \rightarrow \mathrm{NH}_3 + 9\mathrm{OH}^- \qquad (2)$$

$$\mathrm{Al}^{3+} + 3\mathrm{OH}^- \rightarrow \mathrm{Al(OH)}_3\mathrm{(s)} \qquad (3)$$

$$\mathrm{Cr}^{3+} + 3\mathrm{OH}^- \rightarrow \mathrm{Cr(OH)}_3\mathrm{(s)} \qquad (4)$$

The deposits show excellent performance in neutral salt spray test, up to more than 300 hours to first visible red rust for 3 µm thick deposits compared to about 24 hours for pure zinc of the same thickness. The corrosion potentials are similar to the corrosion potentials of pure zinc deposits, which could suggest a non-electrochemical protection mechanism, for example an actual physical blocking of the surface, which inhibits the cathodic and/or anodic reaction to a certain extent.[9]

These processes were developed especially for coil coating in the automotive industry, where high current densities of typically 50-100 A/dm² are required. Therefore, the processes have to be modified to function in the very different conditions of normal decorative zinc plating.

Alternatives to Chromate

In the zinc plating industry there is an increasing demand for alternatives to hexavalent chromate passivation, because of the poisonous nature of Cr(VI) to process workers and to the environment.
There are indeed effective alternatives to chromate passivation, but still they tend to be too expensive for most uses.
A much better way of avoiding chromate passivation would be to incorporate the passivity in the zinc coating itself, and just omit the passivation step.
The first requirement of such a zinc coating is a corrosion resistance comparable to or better than that of chromated zinc.

Experimental Method

The zinc plating in all cases was conducted according to the following procedure:

1. Anodic alkaline degreasing for 3 min. at 5 V.
2. Acid pickling for 1 min.
3. Zinc plating.
4. Drying in pressurized air.

The zinc-plating baths were acid zinc baths containing no additives (table 1, 2). The deposits in all cases had a dull to semi-bright (satin) appearance. As reference coatings for comparison, mirror-bright deposits from a commercial acid chloride zinc bath were used.

Table 1
Plating Conditions for Zn-Al(OH)$_3$-coatings

$ZnCl_2$	50 g/dm^3
H_3BO_3	20 g/dm^3
$Al_2(SO_4)_3$	0-100 g/dm^3
KNO_3	0-0.1 g/dm^3
Temperature	25-50 °C
Current density	0.4-14 A/dm²

Table 2
Plating conditions for Zn-Cr(OH)$_3$-coatings

$ZnSO_4 \cdot 7H_2O$	125 g/dm^3
$(NH_4)_2SO_4$	5-25 g/dm^3
$CrK(SO_4)_2 \cdot 12H_2O$	0.5-3 g/dm^3
KNO_3	0.05-0.75 g/dm^3
Temperature	40-60 °C
Current density	1-10 A/dm²

The zinc plating was performed in a 3 dm^3 glass beaker with magnetic stirring at 600 rpm. The anodes, in all cases, consisted of pure zinc.

For all electrochemical tests and salt spray tests the theoretical layer thickness was 10 μm, calculated for 100 % current efficiency and pure zinc deposition. The layer thickness of Hull cell samples was measured by x-ray equipment.

The substrates for the rotating cylinder Hull cell experiments were mild steel foils.
For electrochemical experiments mild steel cylinders of Ø 1 mm x 1 mm were used.

The neutral salt spray test was performed on mild steel plates of 20 x 20 mm in the case of Zn-Cr(OH)$_3$ coatings and 75 x 50 mm in the case of Zn-Al(OH)$_3$ coatings.

Corrosion Measurements

Electrochemical impedance spectroscopy (EIS) was performed in aerated solution of 3 % NaCl, pH = 6.5. Air was bubbled through the solution for at least 15 min. before immersion of the sample.
The corrosion potential of samples was monitored for at least 15 min. until it was stabilized.

The EIS-measurements were performed at frequencies from 10 kHz-10 mHz, at the corrosion potential and with an amplitude of +/- 10 mV.

After each EIS-measurement, a DC-sweep was performed at a sweep rate of 1 mV/s, from E_{corr} -150 mV to E_{corr} +100 mV.

Neutral salt spray (NSS) test was conducted according to ASTM B117[10] and the samples were rated from 0-10 according to ASTM B537[11], where 10 corresponds to no visible corrosion and 0 corresponds to that more than half of the area is covered by corrosion products.
As no passivation treatment of samples was applied, they were only evaluated with regard to red rust.

Results and discussion

Rotating Cylinder Hull Cell Experiments

Madore et. al.[12] have shown empirically that the current distribution on the rotating cylinder Hull
cell (RCHC, fig. 1) can be expressed as:

$$\frac{i(l)}{i_{av}} = \frac{0.535 - 0.458 \cdot l}{\sqrt{0.0233 + l^2}} + 8.52 \cdot 10^{-5} \cdot e^{7.17 \cdot l} \quad (5)$$

where
l = x/h
x is the distance from the top of the cylinder
h is the height of the cylinder

A series of experiments was performed to confirm this correlation. As seen in fig. 2 the theoretical and the measured results correlate well, except for the upper 10 mm, where all of the measured values are too low. This was caused predominantly by two factors:

1. Shielding of the upper part of the foil due to dendritic growth on the edges.

2. Low current efficiency in the high current density area due to hydrogen evolution.

For the system in question, the RCHC can therefore be trusted to give reliable results from the bottom of the cylinder up to10 mm from the top.

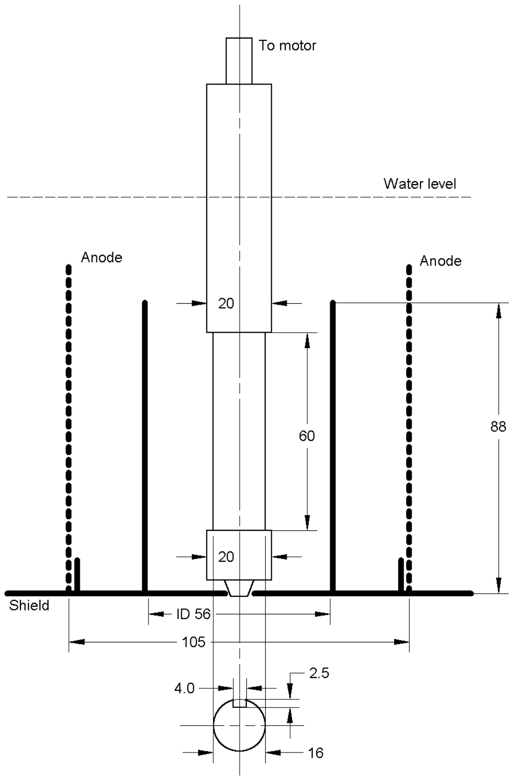

Figure 1. The Rotating Cylinder Hull Cell
All distances in mm

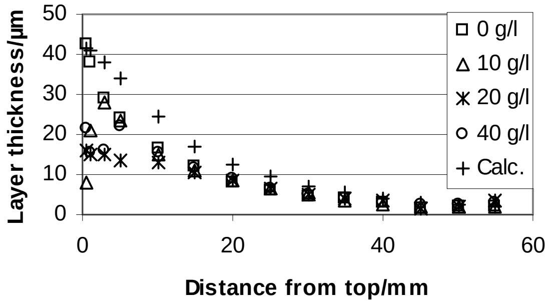

Figure 2. Zn Layer Thickness as a Function of the Distance from Top of RCHC
i-average=2 A/dm², [$Al_2(SO_4)_3$] =0-40 g/l,
T=25 °C, 100 rpm.

Microstructure of Zn-$Al(OH)_3$ coatings

The microstructure of the coatings varied from hexagonal platelets to a spongy morphology depending on the plating parameters. The spongy structures were mainly seen when there was nitrate in the bath but no aluminic ions, which indicates that they were probably caused by the co-deposition of zinc hydroxide (fig. 3a).

The hexagonal platelets were parallel with the substrate at high current densities whilst they were tilted at lower current densities (fig. 3b & d).

In some cases white precipitates were noticed on the hexagonal platelets (fig. 3c), and EDS analyses confirmed that the aluminum content was higher at these points, but it was not possible to perform a quantitative analysis due to the roughness of the precipitates. EDS analysis of the bulk layer revealed an aluminum content of up to 2 wt-% at high current densities (about 7-15 A/dm²), while the contents at lower current densities (about 1-7 A/dm²) were 0.3-0.7 wt-%.

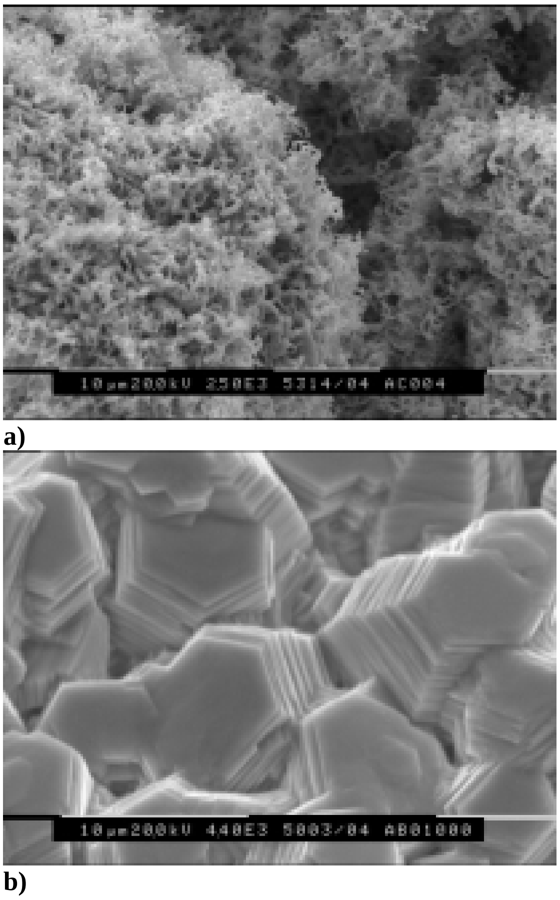

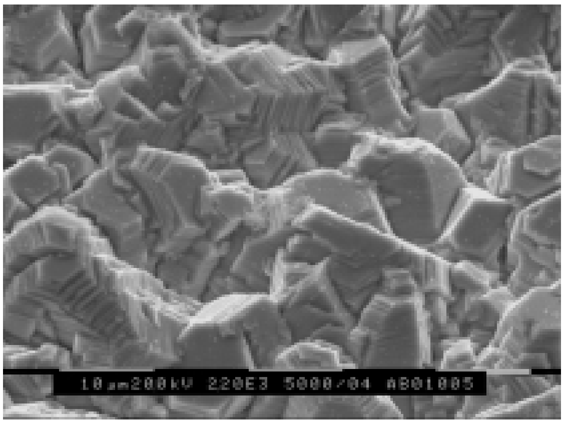

c)

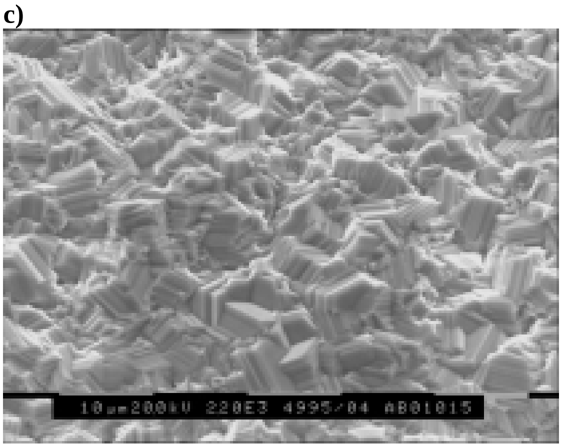

d)

Figure 3. SEM Micrographs of Zn-coatings

- **a) i=2 A/dm², T=50 °C, [KNO_3]=0.05 g/l.**
- **b) i=7 A/dm², T=25 °C, [$Al_2(SO_4)_3$]=40 g/l, 2 wt-% Al**
- **c) i=5.7 A/dm², T=25 °C, [$Al_2(SO_4)_3$]=40 g/l, 2 wt-% Al**
- **d) i=2.9 A/dm², T=25 °C, [$Al_2(SO_4)_3$]=40 g/l, 0.4 wt-% Al.**

Corrosion of Zn-$Al(OH)_3$ coatings

For the Zn-$Al(OH)_3$ coatings, a statistical experimental plan with four factors on three levels was followed (table 3). The design is a Taguchi L_9 orthogonal array and it minimizes the number of experimental runs from eighty-one to nine.

Table 3
Taguchi Experimental Plan

Factor	i	[$Al_2(SO_4)_3$]	[KNO_3]	T
Unit	A/dm²	g/dm^3	g/dm^3	°C
1	1	0	0	25
2	1	50	0.05	40
3	1	100	0.1	50
4	2	0	0.05	50
5	2	50	0.1	25
6	2	100	0	40
7	4	0	0.1	40
8	4	50	0	50
9	4	100	0.05	25

Electrochemical Impedance Spectroscopy

In fig. 4 a typical Nyquist plot is seen. The semicircle indicates a charge-transfer controlled reaction, which means that the polarization resistance equals the charge-transfer resistance, which can be read from the intersection of the semicircle with the x-axis, in this case 540 Ωcm².
The low frequency end of the plot might mark the beginning of a Warburg component indicating a diffusion limited reaction
In some cases, two semicircles are seen more or less overlapping, the last one presumably arising from the formation of a passive layer on the surface of the electrode. In these cases, the polarization resistance is read from the intersection of the second semicircle with the x-axis.

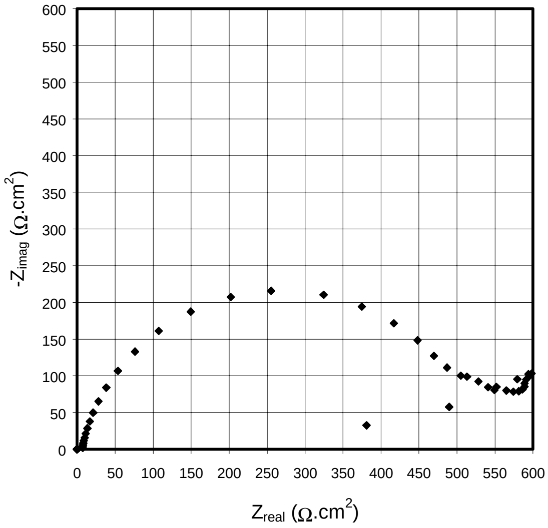

Figure 4. Nyquist plot for zinc coating electroplated at:
i=4 A/dm², [$Al_2(SO_4)_3$]=100 g/dm^3, T=25 °C.

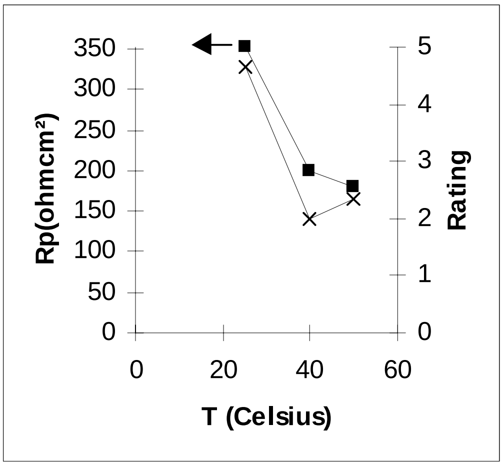

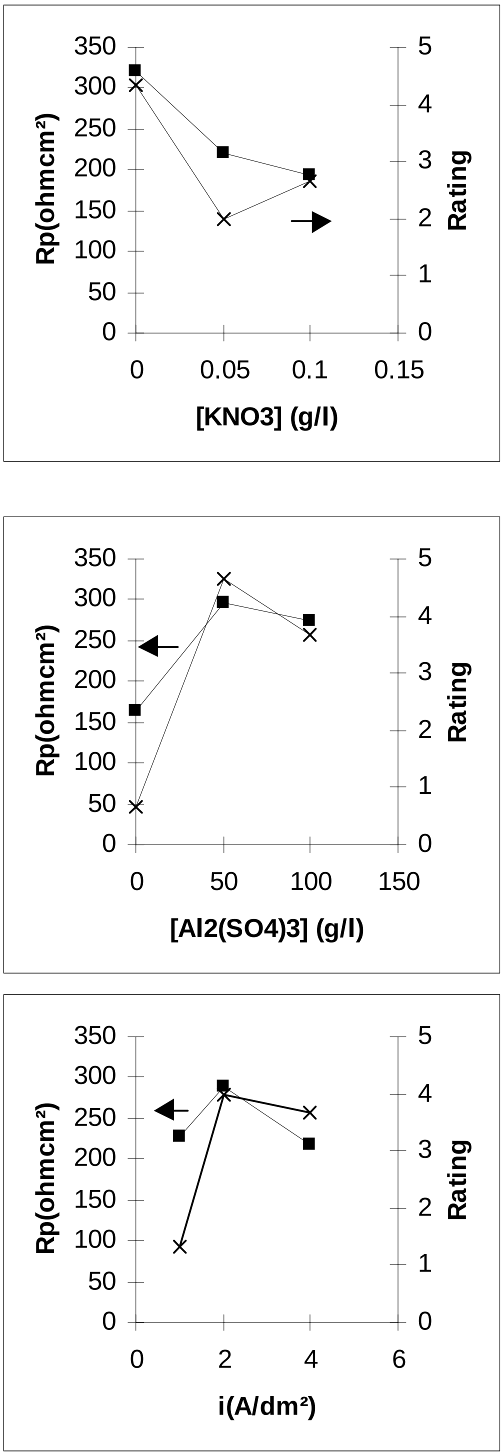

Figure 5. Main Effects Plots for Corrosion Tests. R_p measured by EIS.
Rating in NSS after 168 hours exposure.

In figure 5, the effects of the four parameters are presented. It is seen that the temperature and the concentrations of aluminic ions and nitrate have the largest influence on corrosion resistance, while the effect of current density is much lower. As there are no replications of the experiments, it is not possible to estimate the uncertainty and to perform an analysis of variance (ANOVA). Therefore, a second series of experiments was carried out with three factors on two levels, each performed twice.

The experimental plan, corrosion results and ANOVA-scheme are presented in tables 4 and 5. The F-values must be compared to the fractile F(0.05, 1, 4) = 7.709, and it is now seen that the reproducibility of EIS-measurements is good, and that the concentration of aluminic ions is the only statistically significant factor, while the other factors have no significant effect[13].

The bright zinc reference coating from a commercial zinc bath had a polarization resistance of 330 Ωcm², which is seen from table 4 to be only half the corrosion resistance of the best Zn-$Al(OH)_3$-coatings. The average rating of the reference coatings was 2.5 after 168 hours of NSS, which confirms that the corrosion resistance of the zinc coating was improved by the codeposition of $Al(OH)_3$. EDS-analyses were performed on all coatings, but there was not seen any correlation between the aluminum content and the corrosion resistance. This suggests that other factors such as distribution of particles or texture of the coatings have a major influence on corrosion resistance.

Table 4
Experimental plan for electrochemical corrosion tests.

i A/dm²	$[Al_2(SO_4)_3]$ g/l	$[KNO_3]$ g/l	Rp Ωcm²
4	50	0.1	420, 430
4	100	0	530, 540
8	50	0	340, 370
8	100	0.1	500, 640

Table 5
ANOVA-scheme for corrosion results.

Factor	Dx	Sx	Vx	Fx
i	1	613	613	0.237
$[Al_2(SO_4)_3]$	1	52813	52813	20.4
$[KNO_3]$	1	5513	5513	2.13
Error	4	10350	2588	
Total	7	69288		

Microstructure of Zn-Cr(OH)$_3$ coatings

Preliminary results have shown that the microstructure of Zn-$Cr(OH)_3$-coatings was dendritic at low current densities, but more uniform at higher current densities. To suppress the dendritic growth, the solution was stirred with pressurized air instead of magnetic stirring. This resulted in a much more uniform and better adhering layer.

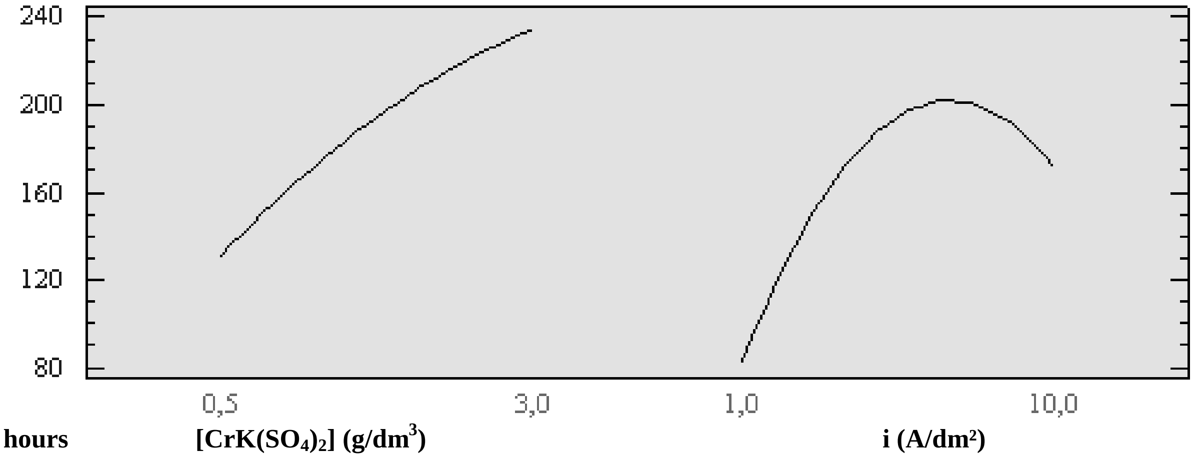

Figure 6. Main effects plot for first appearance of red rust in NSS.

Corrosion of Zn-Cr(OH)$_3$ coatings

For Zn-Cr(OH)$_3$-coatings a Draper-Lin Small Composite experimental design containing twenty-four experiments was used to estimate the effect of five parameters on three levels on the corrosion resistance (table 2).

The concentration of chromic ions and the current density were the only significant factors in this case, while the other factors have only a minor influence on the corrosion resistance (fig. 6).

There was no direct correlation between chromium content and corrosion resistance, which is parallel to the observations made for Zn-Al(OH)$_3$-coatings. The chromium content of the best coatings varied from 2-14 wt-%.

The mirror-bright reference coatings, for comparison, started to show red rust after 96 hours, while the best composite coatings remained free from rust until 264 hours of neutral salt spray testing.

Conclusions

Two types of zinc composite coatings, aluminum hydroxide and chromium hydroxide, were deposited and investigated with respect to corrosion resistance and microstructure.

A considerable improvement of the corrosion resistance in neutral salt spray test was achieved by the codeposition of chromium hydroxide. While the first red rust was observed on the commercial bright zinc coatings after 96 hours the best of the chromium hydroxide coatings lasted 264 hours.

The main effects governing the corrosion resistance were current density and concentration of chromic ions in the plating solution.

The effects of aluminum hydroxide codeposition were somewhat smaller, and the main factor determining corrosion resistance was the concentration of aluminic ions in the plating solution. No direct correlation was found between hydroxide concentration and corrosion resistance, and further investigations of microstructure are required to determine the mechanism behind the improved corrosion resistance.

Acknowledgements

The authors would like to acknowledge funding from the Danish Agency for Trade and Industry, which made this work possible.

References

1. H. Geduld, *Zinc Plating*, Finishing Publications Ltd. (1988).
2. Adaniya Takeshi, Masaru Ohmura, *Interfinish 76*, Proc. of the 9. World congress on metal finishing, Amsterdam, (1976).
3. E. Budman & R. R. Sizelove, *Metal Finishing*, Vol. 96, pp. 324-329 (1998).
4. G. D. Wilcox & D. R. Gabe, *Corrosion Sci.*, Vol. 35, Nos. 5-8, pp. 1251-1258, (1993).
5. W. Kautek, M. Sahre & W. Paatsch, *Electrochimica Acta*, Vol. 39, No. 8/9, pp. 1151-1157 (1994).
6. H. Leidheiser & I. Suzuki, *J. Electrochem. Soc.*, Vol. 128, Is. 2, pp. 242-249 (1981).
7. R. Ramanauskas et Al., *Surface and Coatings Technology*, Vol. 92, pp. 16-21 (1997).
8. H. Leidheiser et Al., *J. Electrochem. Soc.*, Vol. 128, Is. 7, pp. 1456-1459 (1981).
9. K. Mori et al., *Nihon Parkerizing Technical Report*, No. 2 (1989).
10. ASTM standard B 117-94.
11. ASTM standard B 537-70 (86).
12. C. Madore et Al., *Electrochimica Acta*, Vol. 37, No. 1, pp. 69-74 (1992).
13. D.C. Montgomery, *Design and Analysis of Experiments*, John Wiley & Sons, (1991).